DTIC FILE COPY

Naval Research Laboratory
Washington, DC 20375-5000

NRL Memorandum Report 6206

AD-A198 823

Simulation of Electrostatic Modes in a Magnetoplasma with Transverse Inhomogeneous Electric Field

DTIC
ELECTE
AUG 2 4 1988
S D
D

K.-I NISHIKAWA

Department of Physics and Astronomy
The University of Iowa
Iowa City, Iowa 52242

G. GANGULI AND Y.C. LEE*

Science Applications International Corporation
McLean, Virginia 22102

P.J. PALMADESSO

Plasma Physics Division

**University of Maryland*
College Park, MD 20742

May 31, 1988

Approved for public release; distribution unlimited.

88 8 23 048

SECURITY CLASSIFICATION OF THIS PAGE

REPORT DOCUMENTATION PAGE

Form Approved OMB No 0704-0188

1a REPORT SECURITY CLASSIFICATION UNCLASSIFIED	1b RESTRICTIVE MARKINGS
2a SECURITY CLASSIFICATION AUTHORITY 2b DECLASSIFICATION/DOWNGRADING SCHEDULE	3 DISTRIBUTION/AVAILABILITY OF REPORT Approved for public release; distribution unlimited.
4. PERFORMING ORGANIZATION REPORT NUMBER(S) NRL Memorandum Report 6206	5 MONITORING ORGANIZATION REPORT NUMBER(S)
6a. NAME OF PERFORMING ORGANIZATION Naval Research Laboratory 6b OFFICE SYMBOL (If applicable) Code 4780	7a. NAME OF MONITORING ORGANIZATION
6c. ADDRESS (City, State, and ZIP Code) Washington, DC 20375-5000	7b ADDRESS (City, State, and ZIP Code)
8a. NAME OF FUNDING/SPONSORING ORGANIZATION ONR and NASA 8b OFFICE SYMBOL (If applicable)	9 PROCUREMENT INSTRUMENT IDENTIFICATION NUMBER
8c. ADDRESS (City, State, and ZIP Code) 800 N. Quincy Street, Arlington, VA 22203 (ONR) Washington, DC 20546 (NASA)	10 SOURCE OF FUNDING NUMBERS PROGRAM ELEMENT NO 61153N; PROJECT NO W-16-165; TASK NO; WORK UNIT ACCESSION NO DN880-024

11 TITLE (Include Security Classification)
Simulation of Electrostatic Modes in a Magnetoplasma with Transverse Inhomogeneous Electric Field

12 PERSONAL AUTHOR(S)
Nishikawa, K.-I., Ganguli, G. Lee, Y.C. and Palmadesso, P.J.

13a TYPE OF REPORT	13b TIME COVERED	14 DATE OF REPORT (Year, Month, Day)	15 PAGE COUNT
Interim	FROM _____ TO _____	1988 May 31	33

16 SUPPLEMENTARY NOTATION

17 COSATI CODES			18 SUBJECT TERMS (Continue on reverse if necessary and identify by block number)
FIELD	GROUP	SUB-GROUP	Nonuniform Plasma Instability, Nonlocal Simulation, Electrostatic,

19 ABSTRACT (Continue on reverse if necessary and identify by block number)

Ion cyclotron turbulence has been observed with shocks and double layers in the magnetosphere where strongly localized electric fields perpendicular to the magnetic field are present. Theoretical analysis suggests that electrostatic waves with frequency of the order of the ion cyclotron frequency can be destabilized due to the coupling of regions of positive and negative energy ion waves. The nonlocal theory for a smooth profile of transverse inhomogeneous electric fields shows that localized ion waves grow in the region where the electric fields are present. Using a spatially two-dimensional electrostatic code, we investigate this instability in plasma conditions characterized by a localized transverse electric field of width $L << L_x$, where L_x is the simulation length in the x-direction; and distinguish it from the transverse kinetic Kelvin-Helmholtz instability. The simulation results show that the growing ion waves are associated with small vortices at the linear stage, which evolve into a nonlinear stage dominated by larger vortices with lower frequencies. Keywords:

20 DISTRIBUTION/AVAILABILITY OF ABSTRACT ☒ UNCLASSIFIED/UNLIMITED ☐ SAME AS RPT ☐ DTIC USERS	21 ABSTRACT SECURITY CLASSIFICATION UNCLASSIFIED
22a NAME OF RESPONSIBLE INDIVIDUAL J.D. Huba	22b TELEPHONE (Include Area Code) (202) 767-3630 22c OFFICE SYMBOL Code 4780

DD Form 1473, JUN 86 Previous editions are obsolete. SECURITY CLASSIFICATION OF THIS PAGE

S/N 0102-LF-014-6603

CONTENTS

INTRODUCTION.....1

SIMULATION MODEL AND RESULTS.....3

DISCUSSION.....11

ACKNOWLEDGMENTS.....12

REFERENCES.....13

FIGURE CAPTIONS.....14

Accesion For
NTIS CRA&I ☑
DTIC TAB ☐
Unannounced ☐
Justification
By
Distribution /
Availability Codes
Dist | Avail and / or Special
A-1

QUALITY INSPECTED 2

SIMULATION OF ELECTROSTATIC MODES IN A MAGNETOPLASMA WITH TRANSVERSE INHOMOGENEOUS ELECTRIC FIELD

I. INTRODUCTION

The ion-cyclotron instability has been important to both space and laboratory plasmas. In most studies, field-aligned currents or ion beams have served as the driving mechanism.[1] Recently some laboratory experiments[2,3] have reported ion cyclotron instability in circumstances where neither field-aligned currents nor ion beams provide a satisfactory free energy source, and the existence of an inhomogeneous electric field is conjectured to play a role. Furthermore, unstable ion cyclotron waves have been reported in connection with double layers[4] and shocks in space plasmas.[5] In all these cases a localized electric field perpendicular to the ambient magnetic field is an intrinsic feature of the plasma equilibrium.

In order to understand the role of the d.c. electric field in the excitation of the ion waves around the ion cyclotron frequency, Ganguli et al.[6] developed a nonlocal kinetic theory. In the early version of the theory the gradients of the electric field were ignored so as to avoid the confusion with the Kelvin-Helmholtz (K-H) instability which is explicitly dependent on the second derivative of the electric field. They suggested a possible mechanism based on the coupling of positive and negative energy waves, in a plasma equilibrium containing a uniform magnetic field along with a transverse localized electric field, that can excite the ion waves. Dependent on the parameters such as the magnitude of the d.c. electric field, these waves can have real frequencies around the ion cyclotron frequency.

Recently the kinetic theory has been generalized by Ganguli et al[7] to include continuous gradients in the d.c. electric field, and in the weak shear limit (i.e. $V_E'(x)/\Omega_i \ll 1$, where V_E' is the spatial derivative of the E X B drift and Ω is the ion cyclotron frequency) the distinctions between

Manuscript approved February 5, 1988.

the new ion waves and the kinetic K-H waves have been studied. They obtained a general dispersion relation at the second order differential equation level (see the Eq. (29) in Ganguli et al.[7]). For the localized transverse electric field profile ($\sim \mathrm{sech}^2 x$) and the initial density as shown in Fig. 1, the growth rates of the kinetic K-H mode (Fig. 2 (a)) were obtained for various values of $u = k_{\parallel}/k_y$ where $k_{\parallel}$ and k_y are the components of the wave vector in the z (parallel to the magnetic field B_0) and the y directions. The K-H mode is localized below $b = k_y^2\rho_i^2 = 1$ and $k_yL \sim 1$, where L is the scale length associated with the d.c. electric field and $\rho_i = v_{it}/\Omega_i$ is the ion gyro-radius. Furthermore, the growth rates are reduced strongly as u increases. The calculated growth rates of the ion-cyclotron-like modes with $u = 0.038$ are plotted in Fig. 2(b). This mode becomes unstable where $b \gg 1$ and $k_yL \gg 1$. The unstable domains for both modes are clearly distinctive.

In this paper we investigate the new kinetic ion-cyclotron-like (I-C-like) instability[6] driven by a localized electric field perpendicular to the ambient magnetic field by means of particle simulations. The emphasis in this paper is to demonstrate the existence of the new mode[6] and distinguish it from the well known Kelvin-Helmholtz branch and the kinetic modification of this branch. The initial loading of particles in phase space is another significant issue in regard to the simulation of this instability, because the most obvious choice of initial distribution function, i.e., a Maxwellian shifted in the y velocity component due to the E x B drift, is not a self consistent equilibrium. Previous attempts[8] at simulating the IC-like modes have encountered difficulties as a result of this fact. Therefore, we will also attempt to clarify this issue. In Sec II the simulation model and results are presented and concluding remarks and discussions are described in Sec. III.

II. SIMULATION MODEL AND RESULTS

A two-dimensional electrostatic code is used which retains the full dynamics of the ions in three dimensional velocity space. Electrons are treated by the guiding center approximation in the perpendicular direction while the parallel motion is treated exactly. We use a system length $L_x = 128\Delta$, $L_y = 32\Delta$ or 64Δ, where Δ is the grid size which is equal to the electron Debye length, λ_e and $\bar{n}_e\lambda_e^2 = 36$. The external electric field is applied in the form of $E_{ox}(x) = E_{ox}\mathrm{sech}^2[(x - 64)/L]$ in the x-direction which produces E X B drift in the y-direction given by $V_E(x) \approx -E_{ox}(x)/B_o$.

For the present problem, in which a nonuniform d.c. electric field transverse to a uniform magnetic field is present, the initial distribution function constructed out of the constants of motion was provided by Ganguli et al.,[7]

$$f_o(\xi,H) = N \exp(-\beta H)g(\xi) \tag{1}$$

where $N = n_o(\beta/2\pi)^{3/2}$, $\beta = 1/v_t^2, v_t$ is the thermal velocity and

$$g(\xi) = \exp\{\beta[e\Psi(\xi)/m + V_E^2(\xi)/2]\}\eta(\xi)^{-1/2} \tag{2}$$

where $\eta(\xi) = 1+V_E'(\xi)/\Omega$, $[\,]' \equiv d[\,]/d\xi$, $\xi = x+(v_y-V_E(\xi))/\Omega$ is the guiding center position, $H = (v_x^2+v_y^2+v_z^2)/2 + e\Psi(x)/m$ is the total energy and $\Psi(x)$ is the electrostatic potential associated with the d.c. electric field. For the purpose of initial loading in a computer simulation, the

distribution (1) can be expressed in terms of the physical position x (for details see Ganguli et al.[7]),

$$2\pi f_{o\perp} = \frac{\beta \exp\{-\frac{\beta}{2}[v_x^2 + \frac{(v_y - V_E(x))^2}{\eta(x)}]\}}{\sqrt{\eta(x)}} [1 + O(\varepsilon)]. \tag{3}$$

It is interesting to note that the distortion in the gyro-orbit introduced by the sheared transverse d.c. electric field leads to a sustainable difference in the temperature in the two dimensions transverse to the uniform magnetic field. For weak shears (i.e. $V_E'/\Omega << 1$), (3) reduces to

$$2\pi f_{o\perp} = \beta\{1 + \frac{\beta V_E'(x)}{4\Omega}[(v_y - V_E(x))^2 - v_x^2]\} \exp\left(-\frac{\beta}{2}(v_x^2 + (v_y - V_E(x))^2)\right) . \tag{4}$$

We see that for weak shear the use of a shifted Maxwellian for the initial loading is acceptable and the system will adjust to the above distribution automatically with only minor relaxation. If the V_E'/Ω correction is ignored, then (4) becomes identical to a Maxwellian shifted by the magnitude of the E X B drift in the y component of the velocity. Such an initial distribution was used by Pritchett and Coroniti[8] and Pritchett[9] but they extended it to higher shear values ($V_E'/\Omega \geq 1$ so that $\eta \leq 0$) where this initial distribution is no longer acceptable. If the initial state is far from equilibrium then there will be additional artificial free energy which may lead to strong relaxation of the initial nonequilibrium state. Such strong relaxation from a nonequilibrium initial condition is invariably accompanied by a substantial release of free energy, which in turn leads to a noisy dynamic state quite different from

the quiescent initial state essential for simulation of the instability. Therefore, for larger values of V_E'/Ω, the interpretations of the simulation results in these papers[8,9] (especially the conclusion of Pritchett[8], that the Kelvin-Helmholtz instability will always dominate over the new instability[6]) remain dubious.

In the following we shall ignore the order ε terms but retain the shear corrections and employ (3) for the initial loading of our simulations. Later on we shall also use the shifted Maxwellian scheme for a weak and a moderately strong shear case and compare the results with the more appropriate loading scheme given in (3).

We first choose B_{oy}/B_o $(=k_{\parallel}/k_y) = 0.0075$ and $L_y = 64\lambda_e$. The minimum b becomes 0.21. As shown in Fig. 2(a), the kinetic K-H mode has maximum growth rate around b = 0.2. Thus we can expect the simultaneous excitation of both the branches.

Other parameters used are $\Omega_e/\omega_{pe} = 4$, $T_i/T_e = 3.5$, $m_i/m_e = 100$, $L = 11\Delta$, $\alpha = E^2_{0x}/4\pi\bar{n}_e T_e = 0.2$, $V_E^o = 0.59v_{it}$ where $\bar{n}_e$, V_E^o, and v_{it} are the averaged electron density, the peak value of $V_E(x)$ and the ion thermal velocity, respectively. The time evolutions and their spectra are shown for the modes (0, 3) which corresponds to $b = 1.89$, $k_y\rho_i = 1.37$ and $k_yL = 3.23$, and (0,4) which corresponds to $b = 3.38$, $k_y\rho_i = 1.84$ and $k_yL = 4.31$, in Fig. 3. As shown in Fig. 3.(a) the mode (0, 3) begins to grow clearly and emerge from the background thermal noise around $\Omega_i t = 150$, and goes into the nonlinear stage around $\Omega_i t = 300$. The detailed wave analysis shows that in the linear stage this mode has real frequency around $0.5\Omega_i$. As shown in Fig. 3 (b), the peak of the frequency spectrum is located around $0.2\Omega_i$. The frequency of this mode becomes lower in the nonlinear stage. This is a common feature for all the modes. The real frequency of the (0, 4) mode saturates around $0.5\Omega_i$ as shown in Fig. 3 (d). Also from

fig. 3 (b) and (d) we find a number of smaller peaks around higher harmonics.

An estimate of the growth rates of several modes in order to identify the fastest growing mode indicates that the mode (0, 4) which corresponds to b = 3.38, has the maximum growth rate $\gamma/\Omega_i \sim 0.025$. In Fig. 4 we plot the estimated growth rates of the (0,1) to (0,5) modes against b. It should be remarked that the mode (0, 1) which corresponds to b = 0.21 and $k_yL \simeq 1$, and falls on the K-H branch (the solid curve in Fig. 4) has a smaller growth rate ($\gamma/\Omega_i \sim 0.015$) than the higher modes which form the new branch. Clearly it is the ion-cyclotron-like branch with the mode (0,4) that actually dominates. The maximum growth rate of this ion-cyclotron-like mode is located around large b (= 3.38 and $k_yL \sim 4$) and large real frequency ω_r ($\sim \Omega_i$, in the linear stage). Thus, unambiguous distinction is made between the kinetic K-H mode and the new ion-cyclotron-like mode. Besides, we have identified both the branches of the system in our simulation and for the given set of parameters we find that the dominant mode does not belong to the K-H branch; instead it lies on the new I-C-like branch which has higher frequency and shorter wavelength.

The average ion flow velocities $v_y(x)$ are shown in Fig. 5. In the earlier linear stage ($\Omega_i t < 80$) there is hardly any reduction in the peak of the velocity profile or any relaxation in the topology of the profile. In the linear stage we find that the real frequency is around the ion-cyclotron frequency and its higher harmonics. This is in sharp contrast to the simulations of Prichett[8], where there was a strong relaxation of the initial profile right from the very onset of the simulation. The reason for this strong relaxation can be traced to the employment of the simplified initial loading scheme of a shifted Maxwellian in Prichett[8]; which is not acceptable when the magnitude of v_E'/Ω_i is significant. We

discuss the critical importance of the initial loading scheme later on.

In the late quasilinear ($\Omega_i t \approx 250$) and the nonlinear ($\Omega_i t > 300$) stages the wave amplitudes become large and can interact with and reduce the magnitude of the d.c. electric field. Thus in the final stages of the simulation we see a reduction in the magnitude of $V_E(x)$. Also since the real frequency is proportional to $k_y V_E(x)$ (see Ganguli et al.[7]), we find that in the quasilinear stage the real frequency starts reducing along with the magnitude of $V_E(x)$. Further reduction in the real frequency occurs in the fully nonlinear phase.

In the previous simulation we included a slight density gradient. The profile of transverse electric field $E_{ox}(x)/E_{ox}$, the initial density profiles for the electrons and the ions are shown in fig. 6(a), (b), and (c). The density ratio of the maximum to minimum n_h/n_i, equals to 1.1. The density gradients are localized at the half value of the transverse electric field as shown in Fig. 6. The reason that the ion density profile is not as smooth as the electron density profile is due to the fact that the ions have larger gyro-radius. The location of the guiding centers of ions are exactly the same as those of the electrons. However, the gyro-motion of ions smears out the density gradients. This particular profile will be used for all the simulations in this article (except Fig. 7(a) and (b)).

In the preceeding discussions we have established the existence of the I-C-like branch and distinguished it from the K-H branch. We have also demonstrated that at least for some parameters the I-C-like branch can dominate. Hence, in order to economize on the CPU time we shorten L_y to 32Δ in the remainder of this paper to isolate the I-C-like branch and study the characteristic features of this branch only (except Figs. 9 and 11). Note that the mode (0,4) will now correspond to the mode (0,2) and so on.

The time evolutions of the perturbations of the electrostatic potential for the mode (0,2) with and without density gradients and their spectra are shown in Fig. 7. In these cases we use $B_{oy}/B_o = 0.005$, keeping the rest of the parameters unchanged. The case with the density gradients has the growing wave with slightly larger growth rate, larger amplitude, and lower real frequency, as shown in Fig. 7. Inclusion of even a slight density gradient shows enhancement in the growth rate and the amplitude. This is in contrast to the K-H instability where density gradient leads to reduction of the growth rates of the instability[10]. The fact that density gradients lead to stronger growth for the I-C-like modes was predicted by the theory[7].

The dependence of the real frequency ω_r on $V_E(x)$ is now examined. The time evolutions of the perturbations of the electrostatic potential for the mode (0,2) corresponding to $V_E^o = 0.59v_{it}$ and $2.0v_{it}$ and their spectra are shown in Fig. 8. Here $B_{oy}/B_o = 0.005$ and the rest of the parameters remain unchanged. the real frequencies in the linear stages (not necessarily the largest peak) are found around $0.3\Omega_i$ (b) and $1.0\Omega_i$(d). As expected from the theory[7], we find that the real frequencies of the instability are approximately proportional to $k_y V_E^o$.

The diffusion of the guiding center of ions in the case of $L_y = 64\Delta$ is shown at $\Omega_i t = 0$, 80, 160, 240, and 320 in Fig. 9. A subset of ions with initial position such that $58 \leq x \leq 64$, are followed in time, and the local guiding centers of ions are plotted at each time. At the time ($\Omega_i t$=160) when the waves begin to grow out of the thermal noise, slight waving of the column is observed. At the beginning of the nonlinear stage ($\Omega_i t \simeq 240$), the column is twisted. At the nonlinear stage the ions are strongly diffused due to the vortices.

The evolution of vortices at the nonlinear stage ($\Omega_i t \approx 240$) is shown in the case of $L_y = 32\Delta$ in Fig. 10. The electrostatic potential in the x-y plane has strong vortices at the center. The strong vortex moves along the direction of the E x B drift. As shown in Fig. 10, the excited waves are well localized around the center. In the case of $L_y = 64\Delta$ similar strong vortex is also created which moves along the direction of the E x B drift. In the later nonlinear stage the number of the vortices is increased.

The local electric fields $E_{x,y}$ at x = 69, y = 14 in the case of $L_y = 64\Delta$ is diagnosed, and the power spectrum is obtained. As shown in Fig. 11(a), around $\Omega_i t = 300$ strong sharp peaks are produced by the passing vortices. The spectrum has several peaks around Ω_i which correspond to the real frequencies in the linear stage. the largest peak is produced by the vortices in the nonlinear stage.

The profiles of overall wave energy in the case of $L_y = 32\Delta$ are shown in fig. 12. The time-averaged excited wave energy (E_y^2) is localized around the center of the system. Obviously, the excited wave energy is much larger than the thermal energy outside the electric field The time-averaged polarization electric field energy with minus sign $-(E_x)_t^2$ is also plotted, which is much smaller than the excited wave energy.

Now we demonstrate the importance of the proper initial loading. We first examine the weak shear case where $V_E^o/L\Omega = 0.24$, and compare the difference in results produced by the simplified and the improved initial conditions. As expected and noted earlier there is no remarkable difference in the weak shear limit. However, as shown in Fig. 13 (a) and (c) the growth rate of the mode (0, 2) with the improved initial conditions is slightly larger and the amplitudes the nonlinear stage are slightly reduced. Furthermore, at $\Omega_i t = 80$ the average ion flow velocities with our improved initial condition remain almost unchanged whereas the use of the

shifted Maxwellian initial condition leads to relaxation in the velocity profile, although marginal in this case since the shear strength is weak. Apparently, our initial condition improves the simulation results even in the weak shear limit.

The simulations with the larger transverse electric field ($V_E^o = 2.0v_{it}$ which corresponds to $\alpha = 2.24$) with density gradients have been carried out keeping the other parameters the same as in Fig. 13 Now the shear of the d.c. electric field is moderate ($V_E^o/L\Omega_i = 0.86$). Therefore, we expect greater improvements in the simulation results by employing our initial conditions provided in Eq. (3) over the simple initial condition (shifted Maxwellian). Perturbations of electrostatic potential for the mode (0,2) corresponding to the two different initial conditions are compared. As shown in Fig. 14, the mode with our improved initial conditions has much larger growth rate and larger amplitude at the end of the simulation. This demonstrates that with the improved initial condition not only does the initial noise level decreases but also the instability becomes much more coherent and pronounced.

The evolutions of the average ion flow velocities $v_y(x)$ corresponding to the two different initial conditions discussed earlier are also compared for the larger transverse electric field case. As expected, with our initial conditions the early relaxation and reduction of the average ion flow until $\Omega_i t = 80$, was greatly reduced as (see Fig. 15(b)). In this case, the free energy is solely dedicated to excite the large amplitude waves as shown in Fig. 14(c). The amplitudes of the excited waves become quite large at around $\Omega_i t = 240$ and therefore can interact with the d.c. electric field to reduce it's magnitude. At the same time the excited strong vortices cause large diffusions of ions (see Fig. 9(e)) and consequently the average ion flow velocities are greatly reduced.

III. DISCUSSIONS

We have investigated the new ion-cyclotron-like waves driven by a localized transverse electric field by means of a numerical simulation with the assistance of the nonlocal kinetic theory. The linear theory shows that the growth rates of the kinetic Kelvin-Helmholtz modes are strongly reduced with increasing u, and they become unstable only where $b < 1$ and $k_yL \approx 1$. On the other hand, the new modes have larger real frequencies and become unstable at larger $b > 1$ and $k_yL \gg 1$.

We have performed a number of simulations for the new kinetic ion modes. Results show that ion-cyclotron-like waves are excited in the regions where the E X B drift is localized. The linear growth rates of several modes are estimated from the wave analysis of the simulation. This linear analysis shows that the (0, 4) mode which corresponds to large b and large k_yL, has the maximum growth rate. Clearly, these are not K-H modes (See Fig. (2)). Further, the simulation results show that density gradients help to enhance the growth rates. This in in contrast to the established properties of the Kelvin-Helmholtz instability[10]. However, like the K-H mode the real frequencies of this instability are approximately proportional to $k_yV_E^o$. This is predicted by the nonlocal theory.[7]

Furthermore, we established the critical importance of the initial condition which includes the modification due to the gradient of the d.c. electric field.[7] While this improved initial condition is preferable even for weak shears of the d.c. electric field, it becomes crucial when the shear is large. We have demonstrated that for moderate shear values, our initial condition provides the quiescent initial state essential for simulations of the instability. Therefore, the initial relaxation of the average ion flow velocity, which is unavoidable when the simple initial

condition (the shifted Maxwellian) is used for shear values that are significant, is greatly reduced.

The nonlinear phenomena such as diffusion and coalescence of vortices are investigated. In the linear stage, smaller vortices are generated and larger vortices with the lower real frequencies are dominant in the nonlinear stage. In the nonlinear stage the ions diffuse strongly due to the large scale vortices.

ACKNOWLEDGEMENTS

One of the authors (K.-I. N.) would like to thank Prof. L.A. Frank for encouragements. This research was support by NASA, NSF and ONR.

References

1. W.E. Drummond and M.N. Rosenbluth, Phys. Fluids, 5, 1507 (1967
2. M. Nakamura, R. Hatakeyama, and N. Sato, in Proceedings of the Second Symposium on Plasma Double Layers and Related Topics, Innsbruck, Austria, 1984, (Institute for Theoretical Physics, University of Innsbruck, Innsbruck, 1984), p. 171.
3. N. Sato, M. Nakamura, and R. Hatakeyama, Phys. Rev. Lett., 57, 1227 (1986).
4. R.L. Merlino, S.L. Cartier, M. Alport, and G. Knorr,in Proceedings of the Second Symposium on Plasma Double Layers and Related Topics, Innsbruck, Austria, 1984, (Institute for Theoretical Physics, University of Innsbruck, Innsbruck, 1984), p. 224.
5. F.S. Mozer, C.W. Carlson, M.K. Hudson, R.B. Torbert, B. Parady, J. Yatteau and M.C. Kelly, Phys. Rev. Lett., 38, 292, (1977); M. Temerin, C. Cattel, R. Lysak, M. Hudson, R.B. Torbert, F.S. Mozer, R.D. Sharp, and P.M. Kinter, J. Geophys. Res., 86, 11278 (1981).
6. G. Ganguli, Y.C. Lee, and P. Palmadesso, Phys. Fluids, 28, 761, (1985); G. Ganguli, P. Palmadesso, and Y.C. Lee, Geophys. Res. Lett., 12, 643 (1985).
7. G. Ganguli, Y.C. Lee, and P.J. Palmadesso, Phys. Fluids, 31, 823 (1988).
8. P.L. Pritchett, Phys. Fluids, 30, 272 (1987).
9. P.L. Pritchett and F.V. Coroniti, J. Geophys. Res., 89, 168 (1984).
10. P. Satyanarayana, Y.C. Lee, and J.D. Huba, Phys. Fluids, 30, 81 (1987).

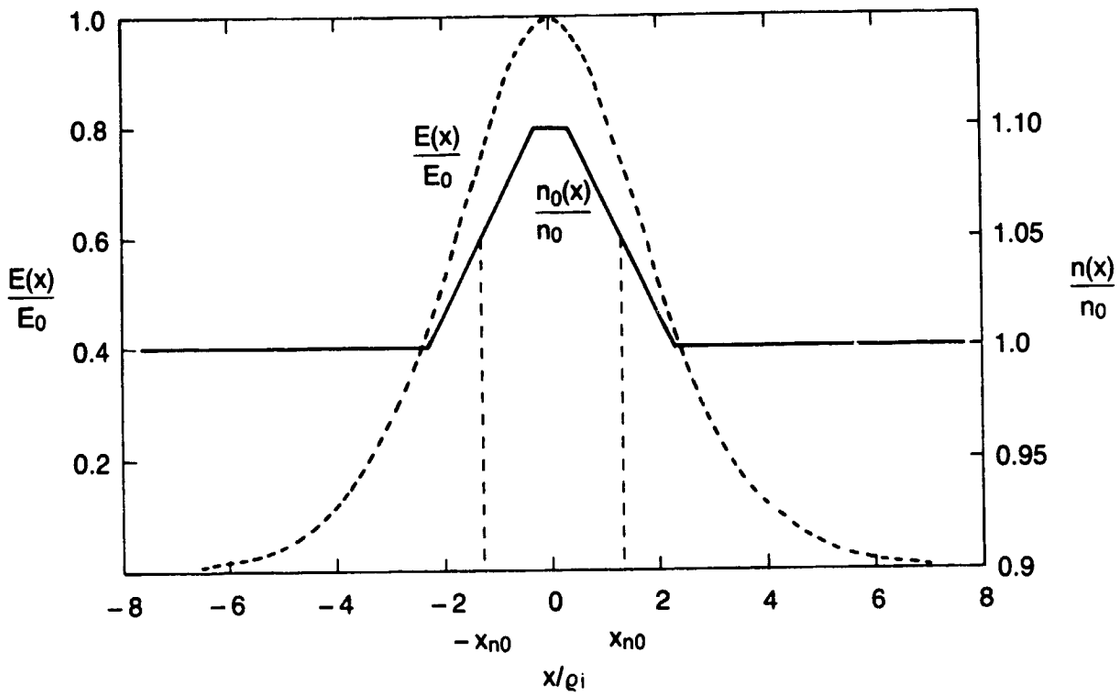

Fig. 1. The profile of the transverse electric field and density used for the nonlocal theoretical analysis.

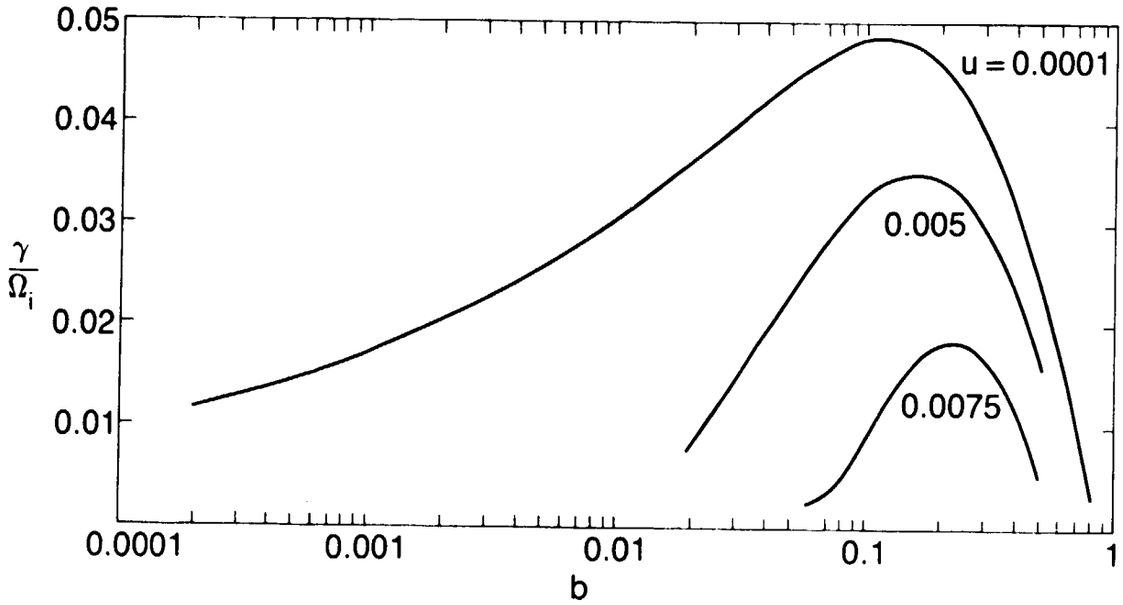

Fig. 2 (a) The extended version for the growth rates of the Kelvin-Helmholtz mode with $u = k_{\parallel}/k_y = 0.0001$, 0.005, and 0.0075.

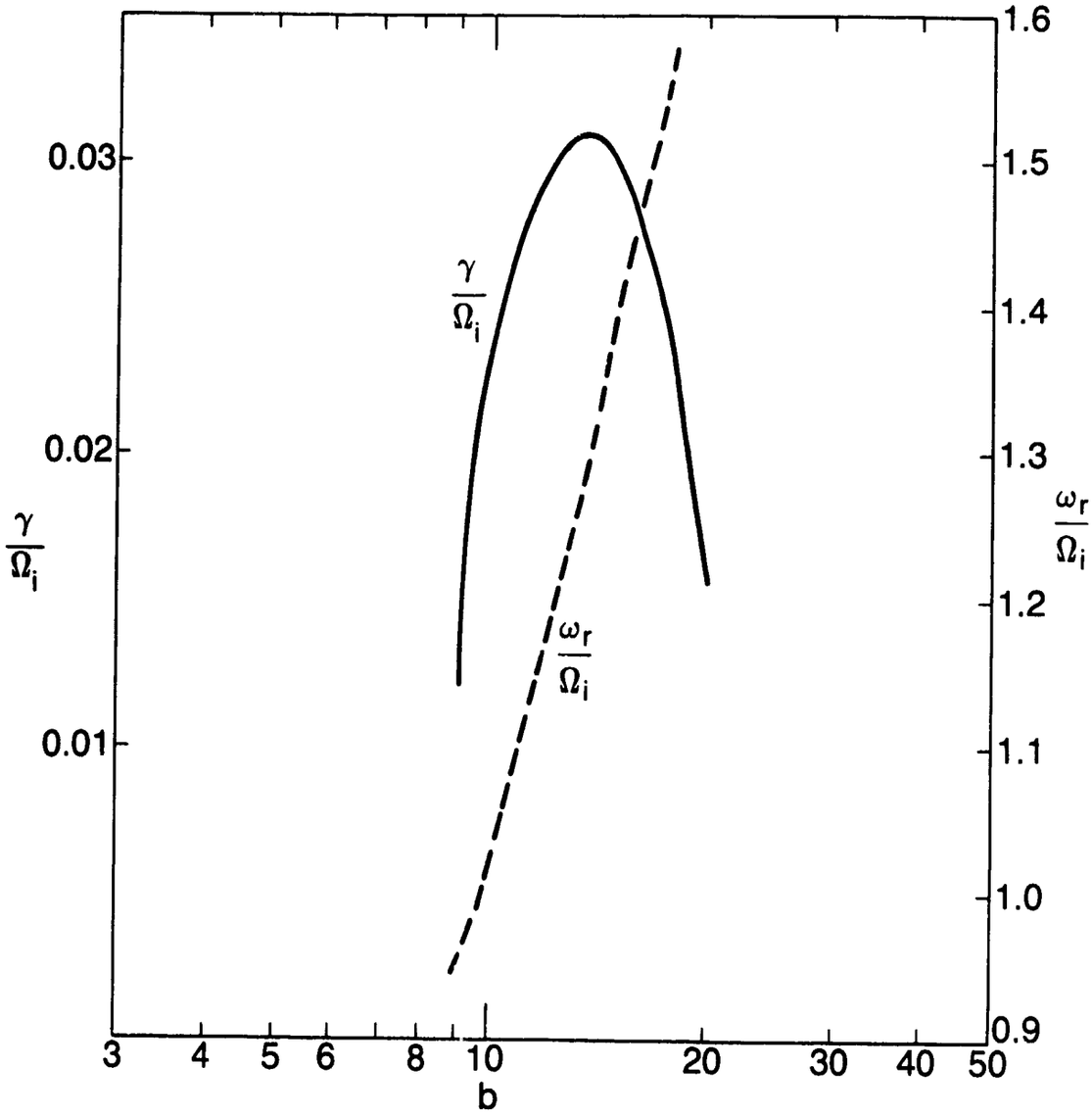

Fig. 2 (b) The growth rate of the Kelvin-Helmholtz mode and the real and imaginary frequencies of the ion-cyclotron-like mode with $u = k_{\parallel}/k_y = 0.038$ and the simulation results with $B_{yo}/B_o = 0.0075$.

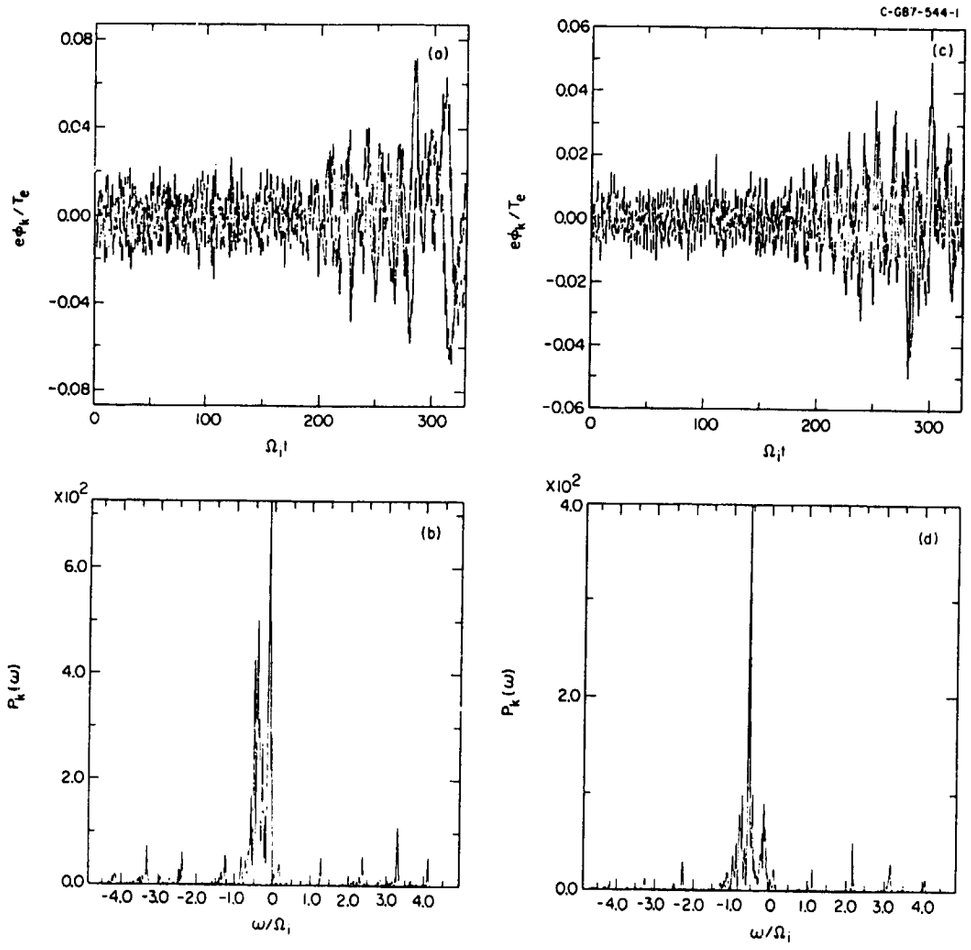

Fig. 3. The time evolutions ((a), (c) and their power spectra (b), (d)) of the perturbations of electrostatic potential for two modes in the case of $L_y = 64\Delta$ with the slight density gradients.

(a), (b): $k_{\parallel}/\lambda_{e\parallel} = 0.0075 \times 2\pi \times 3/64 = 2.21 \times 10^3$, $k_y\lambda_{e\parallel} = 2\pi \times 3/64 = 0.295$.

(c), (d): $k_{\parallel}/\lambda_{e\parallel} = 0.0075 \times 2\pi \times 4/64 = 2.95 \times 10^3$, $k_y\lambda_{e\parallel} = 2\pi \times 4/64 = 0.393$.

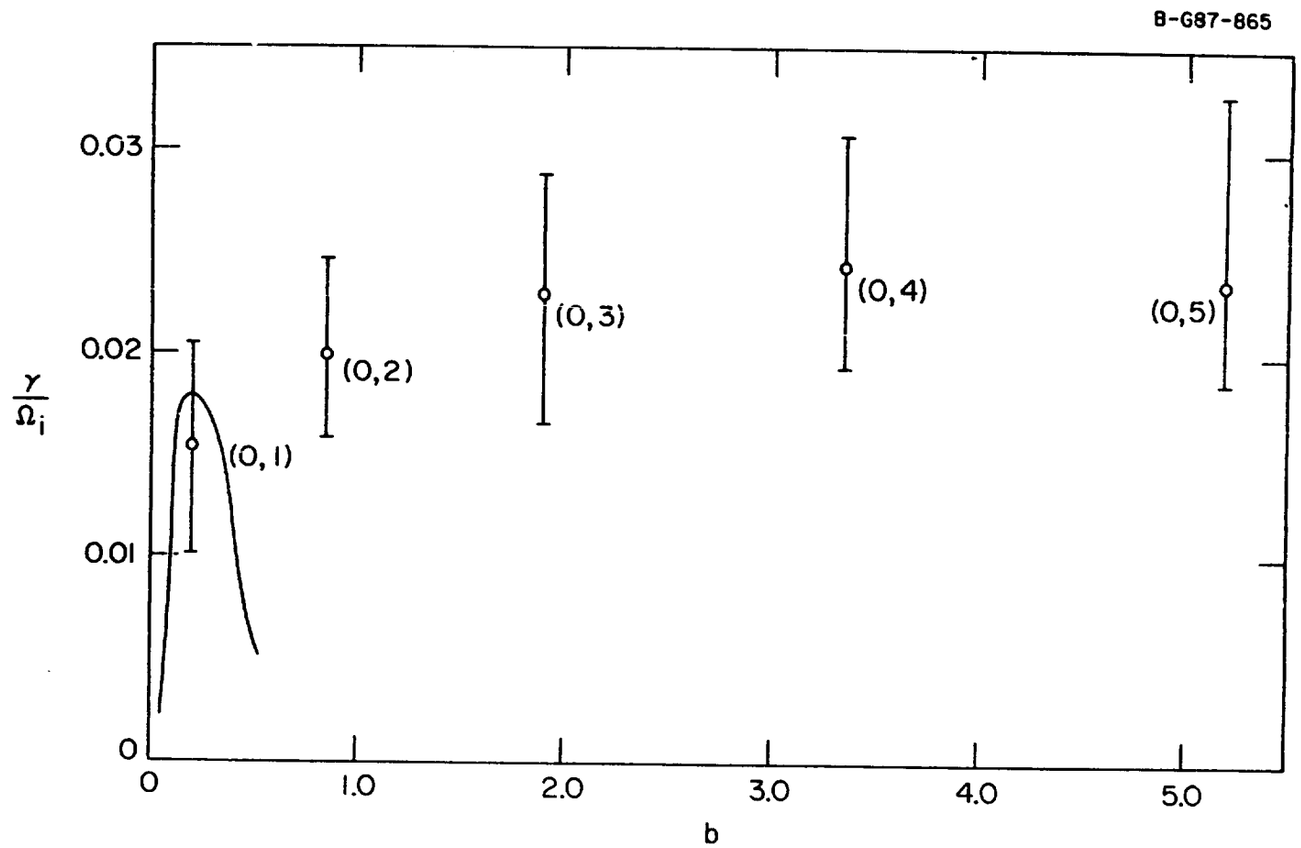

Fig. 4. The estimated growth rates of the (0,1) to (0,5) modes as obtained from the simulation described in Fig. 3. The solid curve is the theoretically predicated Kelvin-Helmholtz branch for identical parameters.

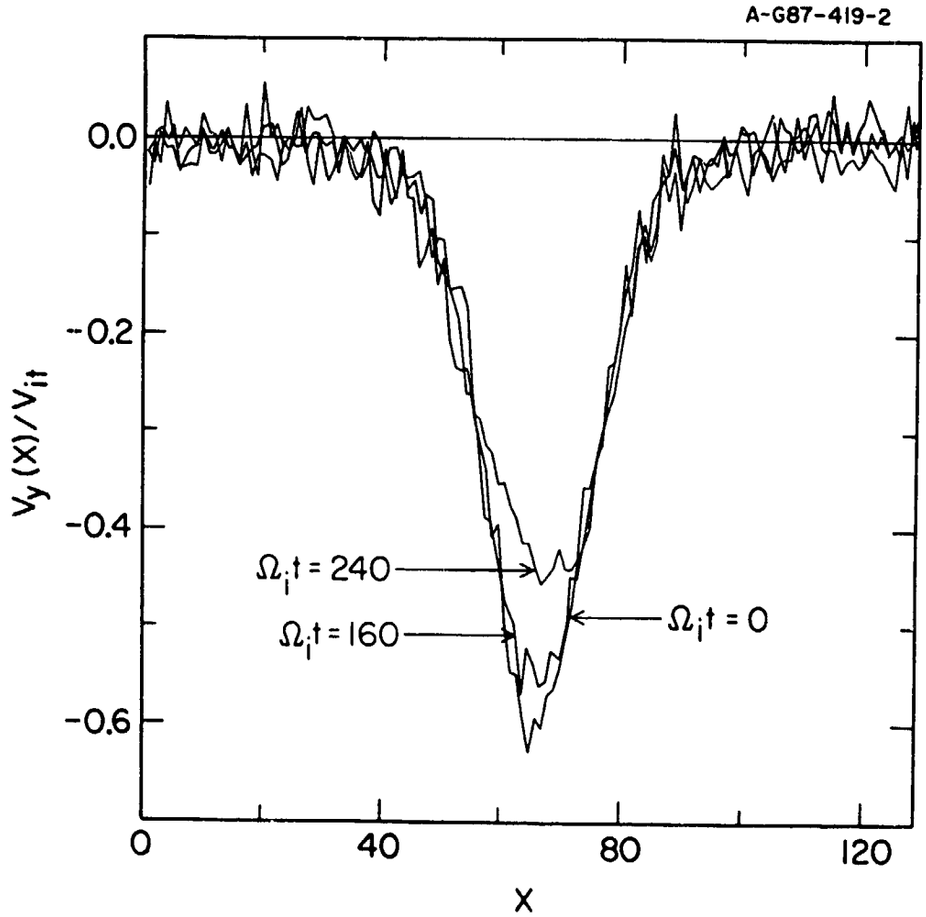

Fig. 5. The average ion flow velocity $v_y(x)$ at $\Omega_i t$ = 0, 160 and 250 in the same case as Fig. 3.

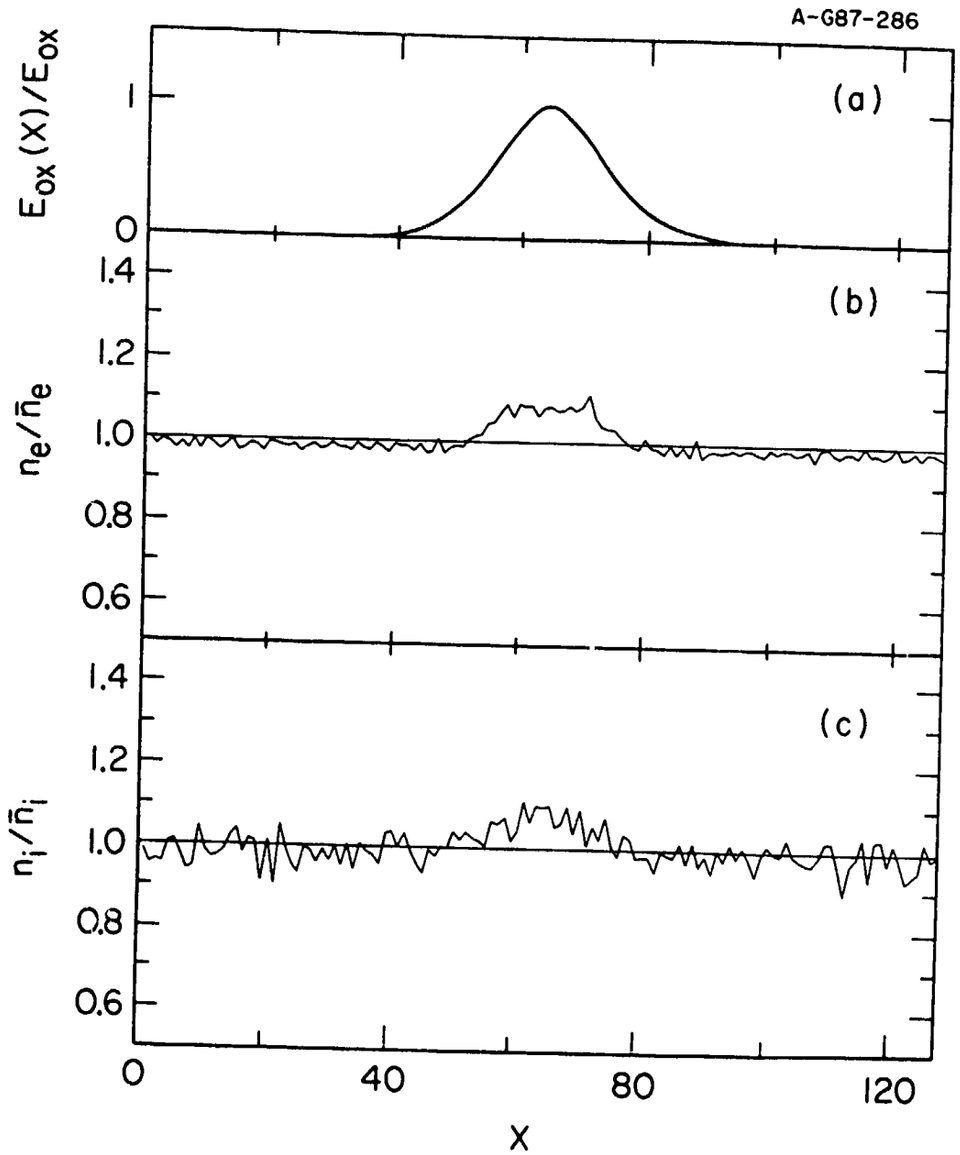

Fig. 6. The profile of the transverse electric field (a), electron density (b), and the ion density (c) with the density gradients at $\Omega_i t = 0$.

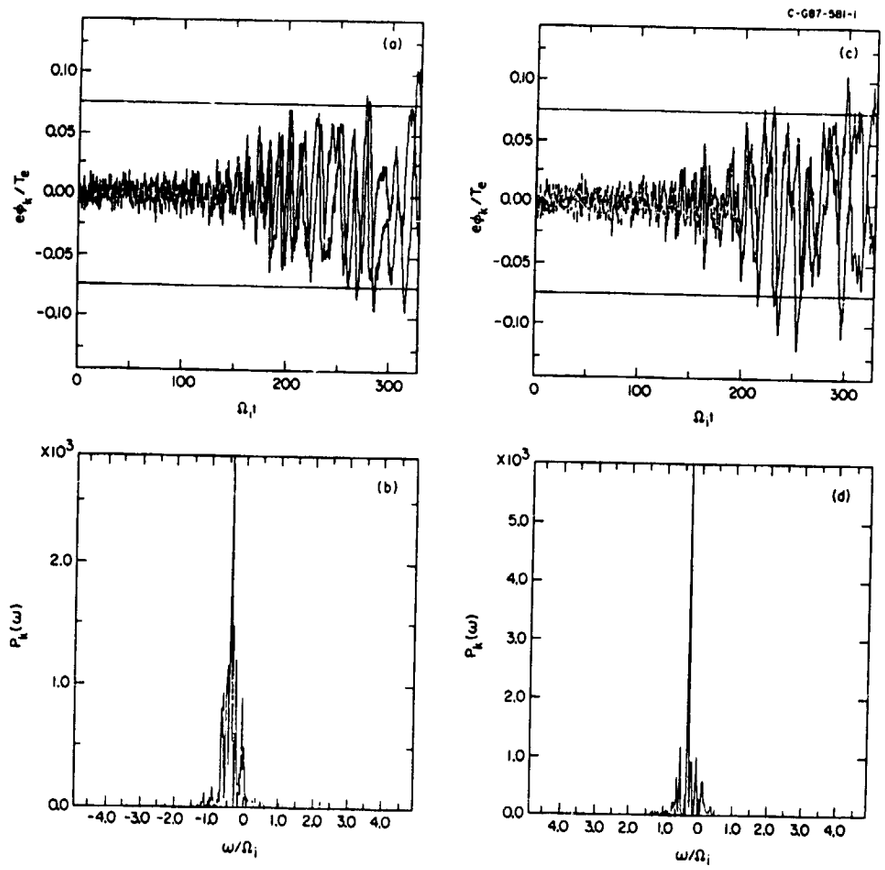

Fig. 7. The time evolution of perturbations of electrostatic potential of the (0, 2) mode in the case of $L_y = 32\Delta$ ((a), (c)) and their power spectra (b), (d)), ($V_E^o = 0.59\ V_{it}$, $B_{oy}/B_o = 0.005$).

(a), (b): no density gradient

(c), (d): with the gradients.

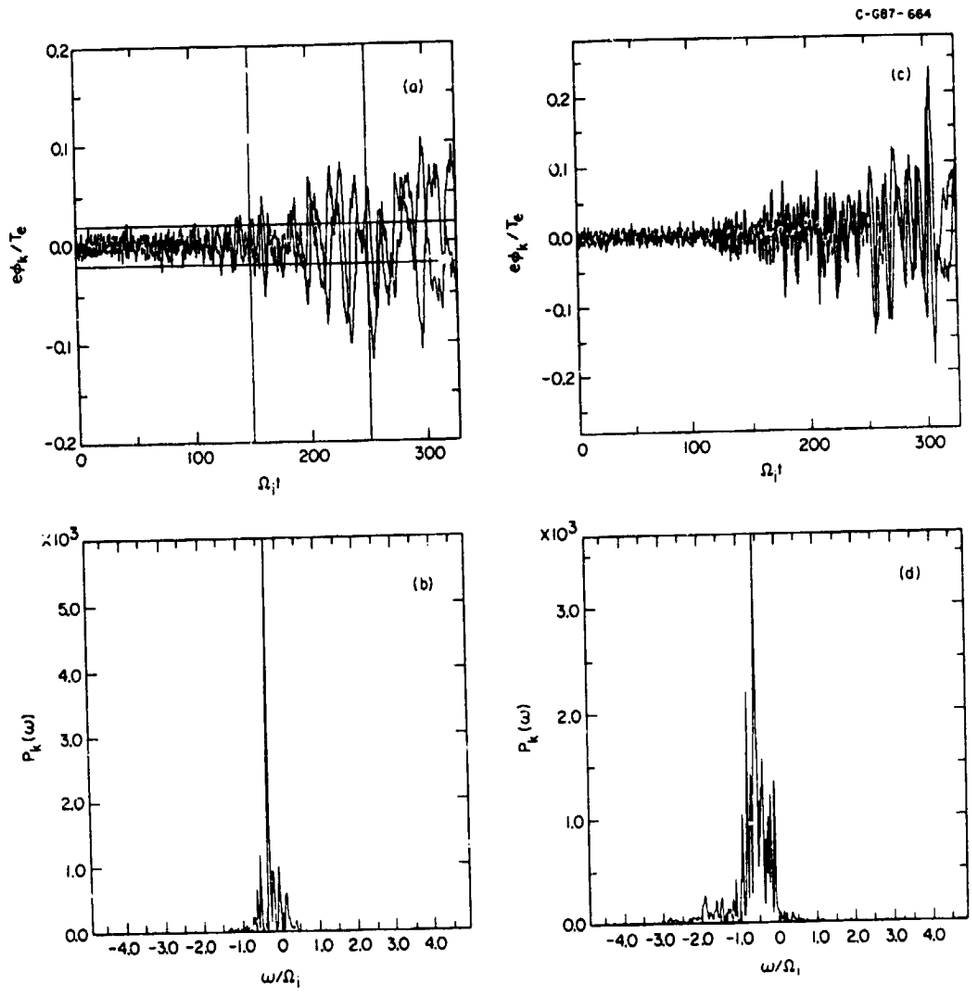

Fig. 8. The dependence of the real frequency on the V_B^o. The time evolutions of perturbations of electrostatic potential of the mode (0,2) in the case of $L_y = 32\Delta$

((a), (c)) and their power spectra ((b), (d)) $(B_{oy}/B_o = 0.005$.

(a), (b): $V_E^o = 0.59v_{it}$.

(c), (c): $V_E^o = 2.0v_{it}$.

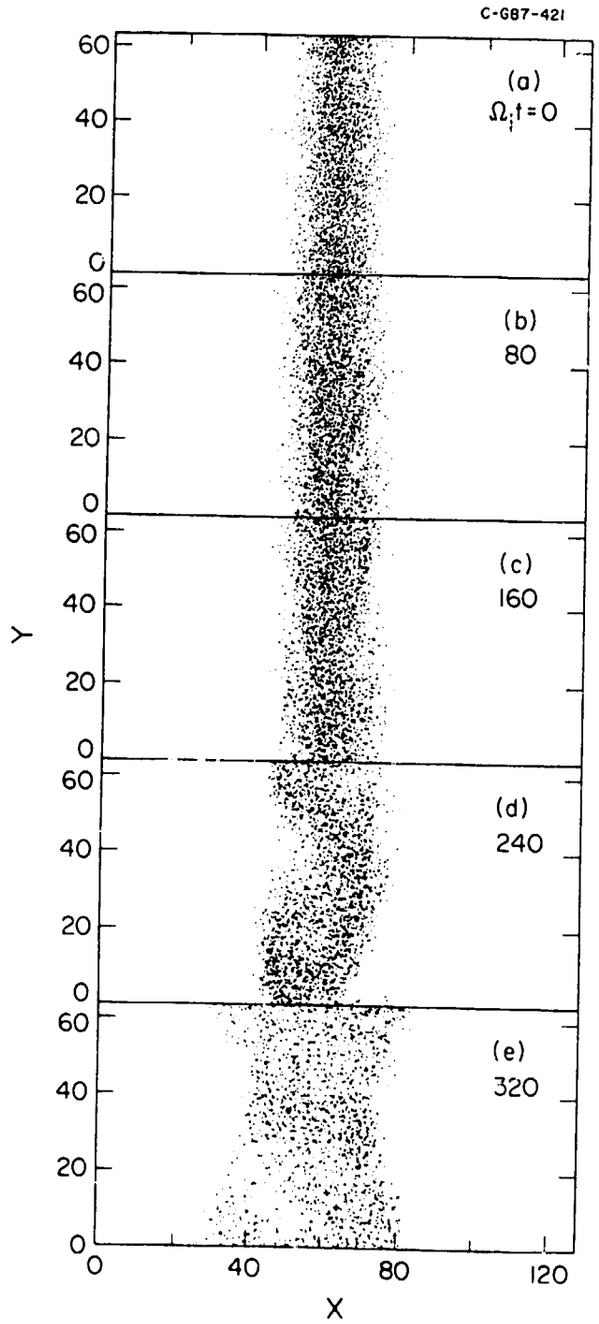

Fig. 9. The diffusion of the gryo-center of ions whose initial actual positions are $58 \leq x \leq 64$ at $\Omega_i t = 0, 80, 160, 240$, and 320 in the same case as fig. 3 ($L_y = 64\Delta$).

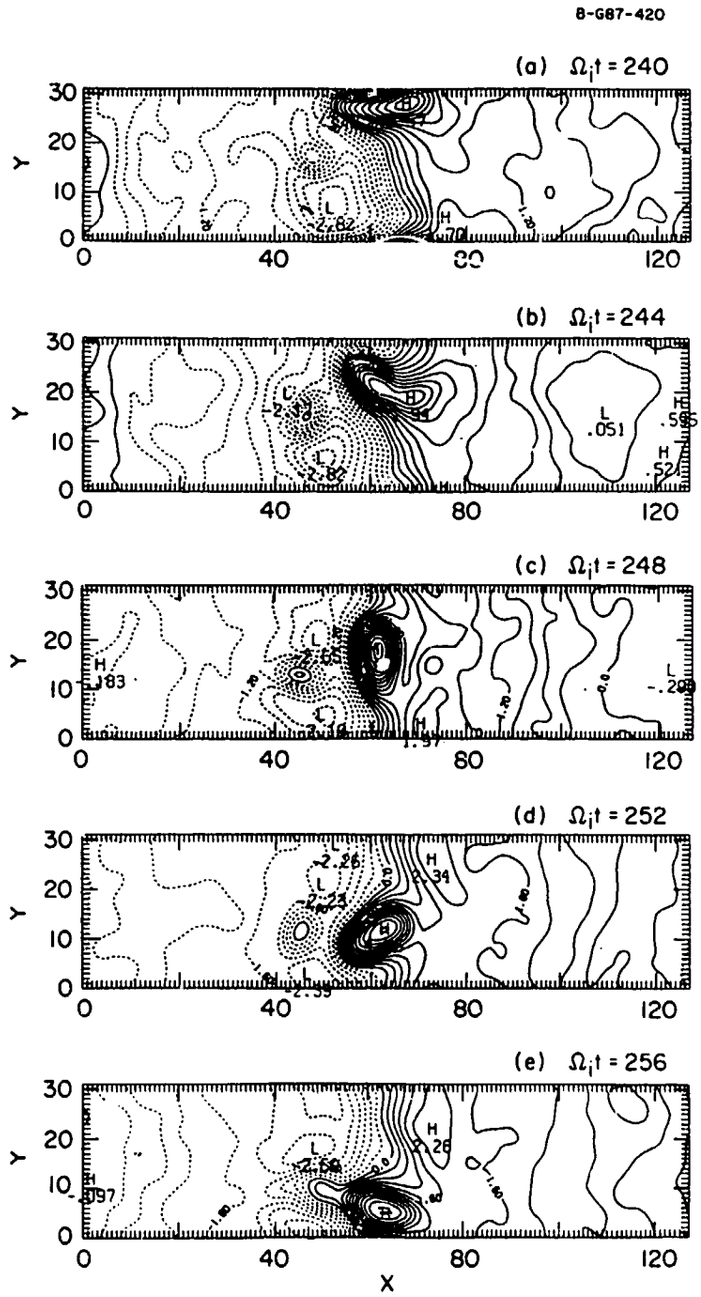

Fig. 10. The time evolution of the contour plots of the electrostatic potential at the nonlinear stage in the case of $L_y = 32\Delta, B_{oy}/B_o = 0.075$.

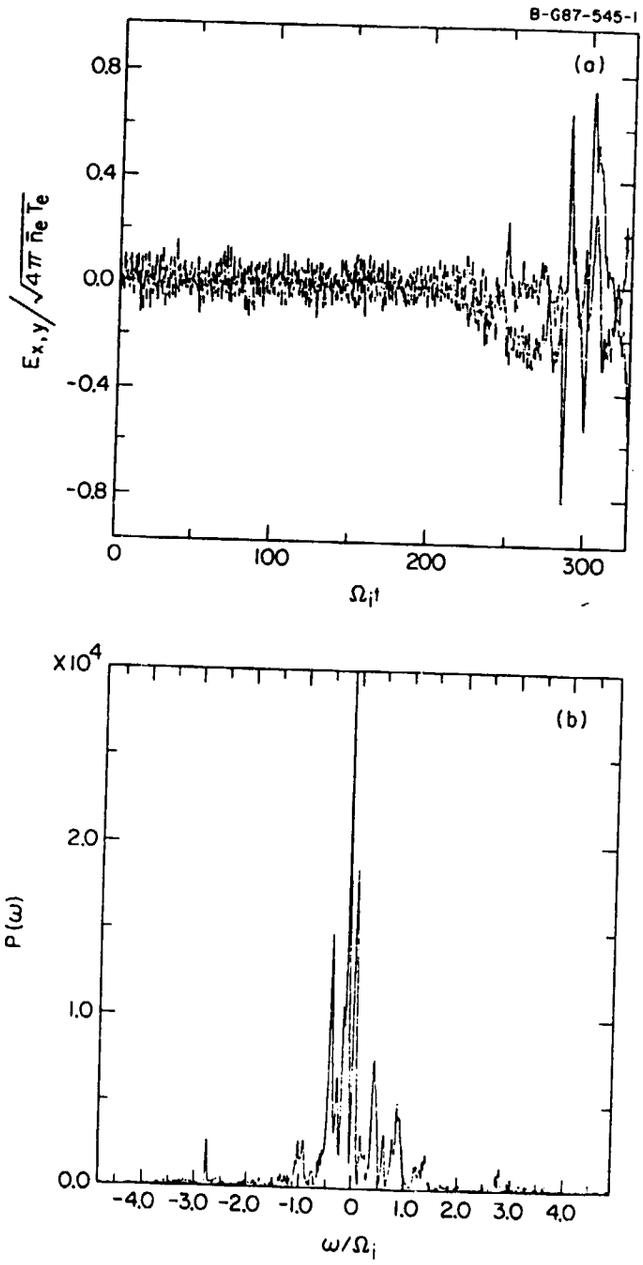

Fig. 11 The time evolution of local electric field $E_{x,y}$ at x = 69, y = 14 (a) and it power spectrum (b) in the same case as Fig. 3 (L_y = 64Δ).

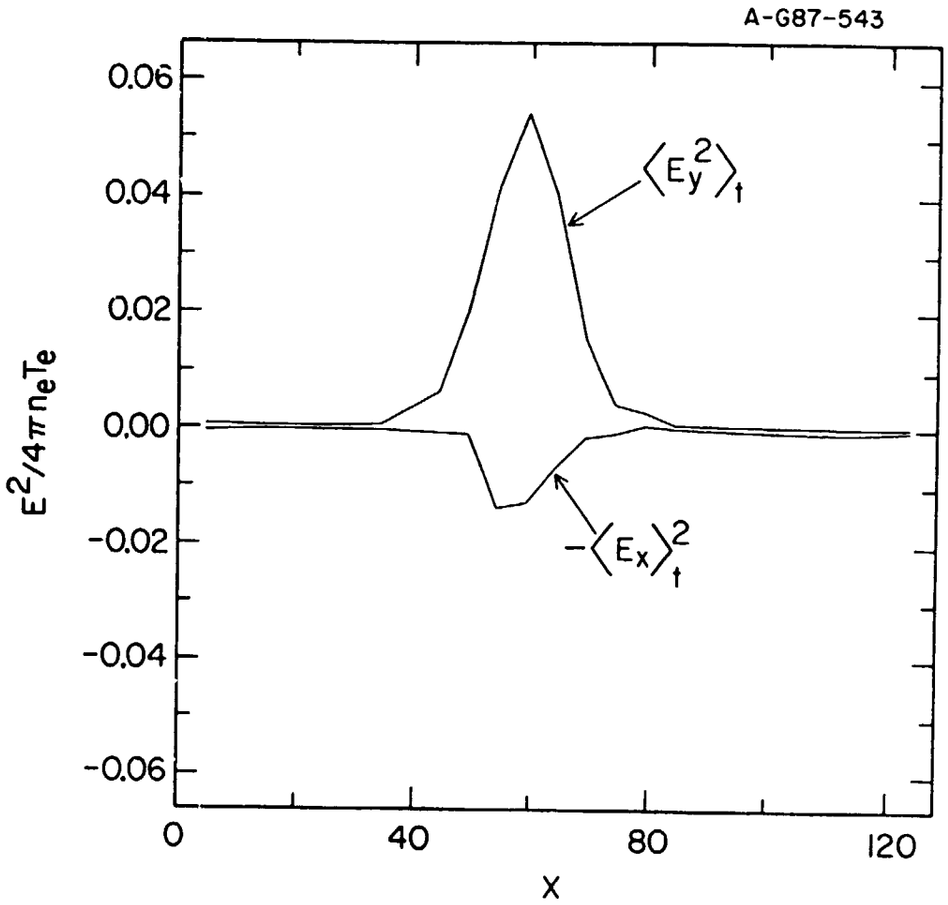

Fig. 12. The averaged field energy $\langle E_y^2 \rangle t$ and the d.c. type polarized electric field energy $-\langle E_x \rangle_t^2$ are localized around the center in the case of $L_y = 32\Delta, B_{oy}/B_o = 0.0075$.

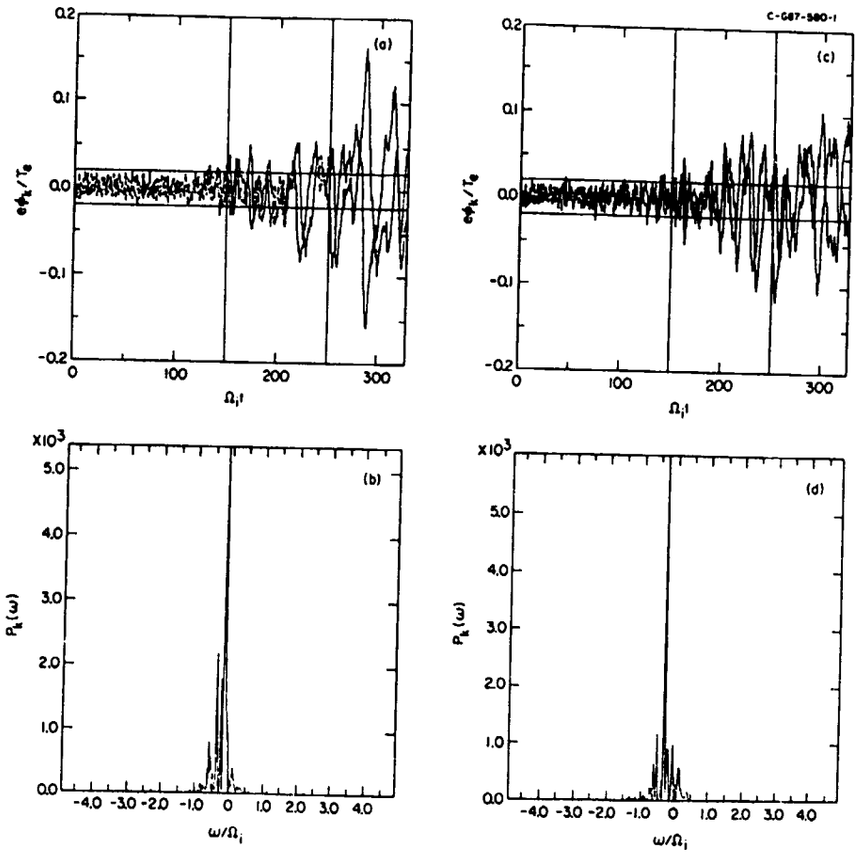

Fig. 13. Comparison of the results with two different initial conditions with density gradients as shown in Fig. 5 (The mode (0,2) in the case of $L_y = 32\Delta, B_{py}/B_o = 0.005$).

(a),(b): the simplified initial condition.

(c),(d): the improved initial condition.

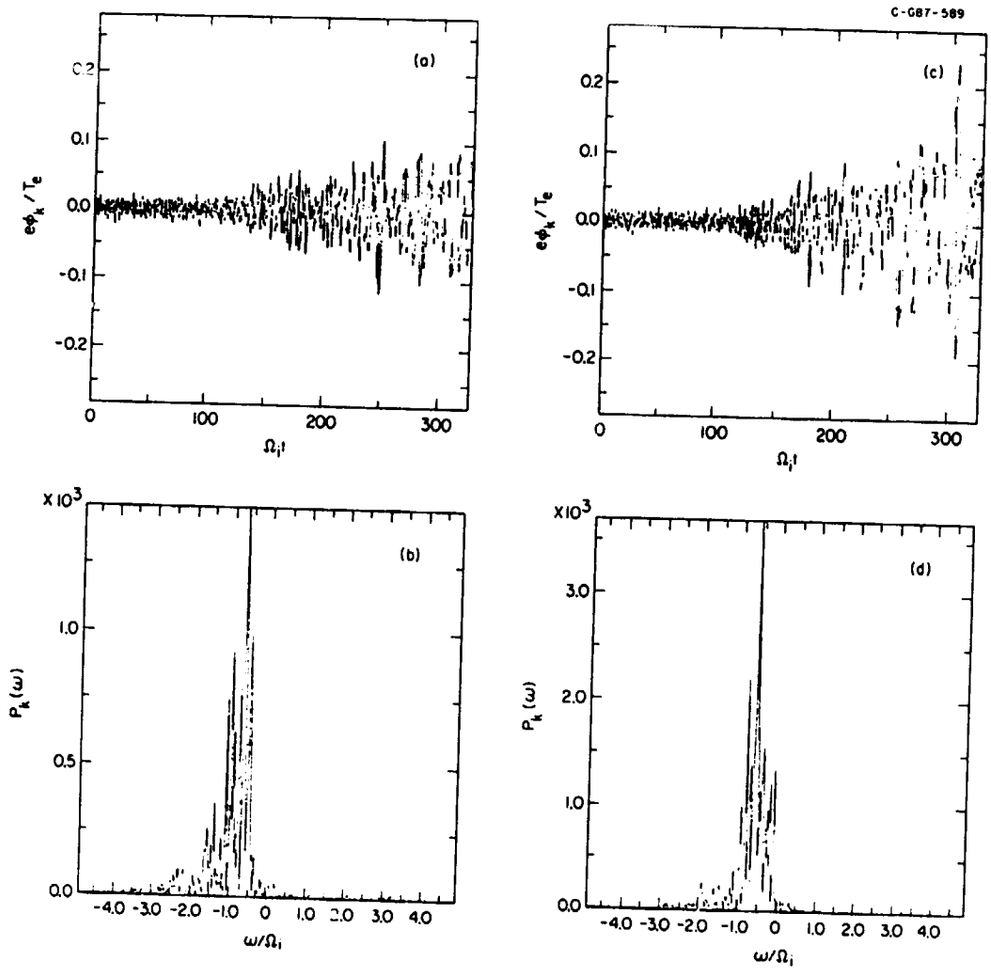

Fig. 14. The time evolution of perturbation of electrostatic potential ((a), (c)) and their power spectrum ((b), (d)) in the case of $\alpha = E_{ox}^2/4\pi\bar{n}_e T_e = 2.24$, $v_E^o = 2.0v_{it}$, $k_{\parallel}\lambda_{e\parallel} = 0.005 \times 2\pi \times 2/32 = 1.96 \times 10^{-3}$, and $k_y\lambda_{e\parallel} = 2\pi/32 = 0.393$.

(a),(b): the simplified initial conditions.

(c),(d): the improved initial conditions.

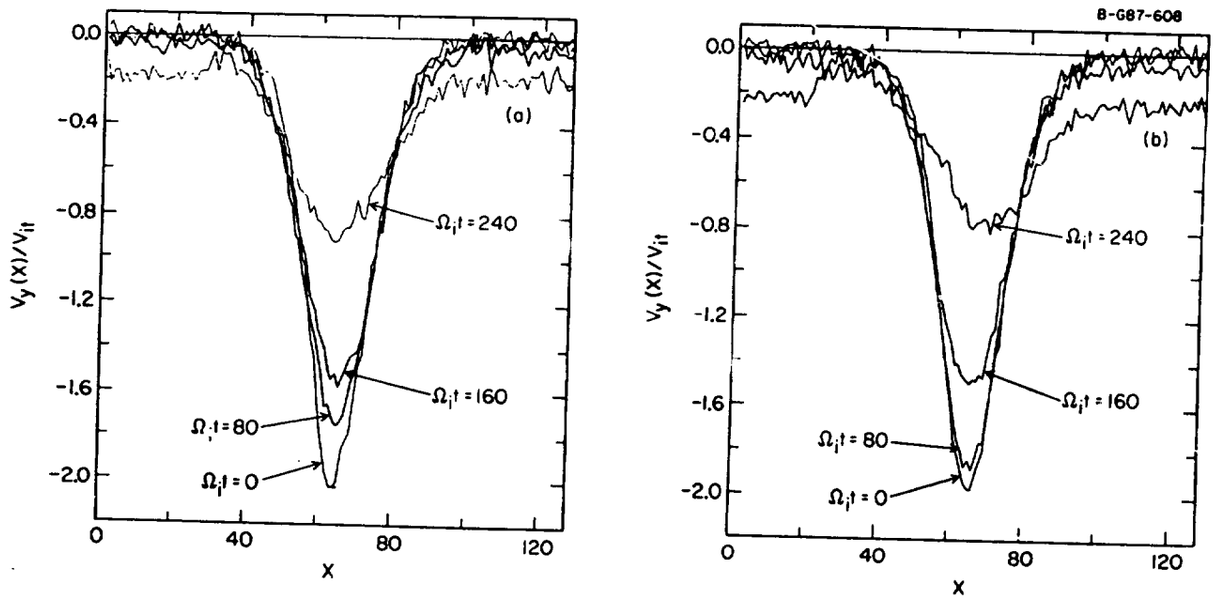

Fig. 15. The evolutions of the average ion flow velocities $v_y(x)$ in the cases of the larger transverse electric fields as same as in Fig. 13.

(a): the simplified initial conditions.

(b): the improved initial conditions.

DISTRIBUTION LIST
(Unclassified Only)

DISTRIBUTE ONE COPY EACH TO THE FOLLOWING PEOPLE (UNLESS OTHERWISE NOTED)

DIRECTOR
NAVAL RESEARCH LABORATORY
WASHINGTON, DC 20375-5000
CODE 4700 (26 CYS)
CODE 4701
CODE 4780 (50 CYS)
CODE 4750 (P. RODRIGUEZ)

OFFICE OF NAVAL RESEARCH
WASHINGTON, DC 22203
C. ROEERSON

DIRECTOR
DEFENSE NUCLEAR AGENCY
WASHINGTON, DC 20305
L. WITTWER
B. PRASAD

COMMANDING OFFICER
OFFICE OF NAVAL RESEARCH
WESTERN REGIONAL OFFICE
1030 EAST GREEN STREET
PASADENA, CA 91106
R. BRANDT

NASA HEADQUARTERS
CODE EE-8
WASHINGTON, DC 20546
S. SHAWHAN
D. BUTLER

NASA/GODDARD SPACE FLIGHT CENTER
GREENBELT, MD 20771
M. GOLDSTEIN, CODE 692
R.F. BENSON, CODE 692
T. NORTHROP, CODE 665
T. BIRMINGHAM, CODE 695.1
A. FIGUERO VINAS, CODE 692
SHING F. FUNG, CODE 696
D.S. SPICER, CODE 682

AEROSPACE CORPORATION
A6/2451, P.O. BOX 92957
LOS ANGELES, CA 90009
A. NEWMAN
D. GORNEY
M. SCHULZ
J. FENNEL

BELL LABORATORIES
MURRAY HILL, NJ 07974
A. HASEGAWA
L. LANZEROTTI

LAWRENCE LIVERMORE LABORATORY
UNIVERSITY OF CALIFORNIA
LIVERMORE, CA 94551
LIBRARY
B. KRUER
J. DEGROOT
B. LANGDON
R. BRIGGS
D. PEARLSTEIN

LOS ALAMOS NATIONAL LABORATORY
P.O. BOX 1663
LOS ALAMOS, NM 87545
S.P. GARY
N. QUEST
J. BRACKBILL
J. BERN
J. BOROVSKY
D. FORSLUND
B. BEZZERIDES
C. NIELSON
D. RIGGIN
D. SIMONS
L. THODE
D. WINSKE

LOCKHEED RESEARCH LABORATORY
PALO ALTO, CA 94303
M. WALT
J. CLADIS
Y. CHIU
R. SHARP
E. SHELLEY

NATIONAL SCIENCE FOUNDATION
ATMOSPHERIC RESEARCH SECTION
WASHINGTON, DC 20550
D. PEACOCK

PHYSICAL INTERNATIONAL CORP.
2400 MERCED STREET
SAN LEANDRO, CA 94557
J. BENFORD
S. STALINGS
Y. YOUNG

SANDIA LABORATORIES
ALBUQUERQUE, NM 87115
A. TOEPFER
D. VANDEVENDER
J. FREEMAN
T. WRIGHT

SCIENCE APPLICATIONS
INTERNATIONAL CORPORATION
LAB. OF APPLIED PLASMA STUDIES
P.O. BOX 2351
LAJOLLA, CA 92037
L. LINSON

TRW SPACE AND TECHNOLOGY GROUP
SPACE SCIENCE DEPARTMENT
BUILDING R-1, ROOM 1170
ONE SPACE PARK
REDONDO BEACH, CA 90278
R. FREDERICKS
W.L. TAYLOR

UNIVERSITY OF ALASKA
GEOPHYSICAL INSTITUTE
FAIRBANKS, AK 99701
LIBRARY
S. AKASOFU
J. KAN
J. ROEDERER
L. LEE
D. SWIFT

UNIVERSITY OF ARIZONA
DEPT. OF PLANETARY SCIENCES
TUCSON, AZ 85721
J.R. JOKIPII

BOSTON COLLEGE
DEPARTMENT OF PHYSICS
CHESTNUT HILL, MA 02167
R.L. CAROVILLANO
P. BAKSHI

UNIVERSITY OF CALIFORNIA, S.D.
LAJOLLA, CA 92037
(PHYSICS DEPARTMENT):
T. O'NEIL
J. WINFREY
LIBRARY
J. MALMBERG
(DEPT. OF APPLIED SCIENCES):
H. BOOKER

UNIVERSITY OF CALIFORNIA
SPACE SCIENCE LABORATORY
BERKELEY, CA 94720
M. TEMERIN
F. MOZER

UNIVERSITY OF CALIFORNIA
PHYSICS DEPARTMENT
IRVINE, CA 92664
LIBRARY
G. BENFORD
N. ROSTOKER
C. ROBERTSON
N. RYNN

UNIVERSITY OF CALIFORNIA
LOS ANGELES, CA 90024
(PHYSICS DEPARTMENT):
J.M. DAWSON
B. FRIED
J. MAGGS
J.G. MORALLES
W. GEKELMAN
R. STENZEL
Y. LEE
A. WONG
F. CHEN
M. ASHOUR-ABDALLA
LIBRARY
J.M. CORNWALL
R. WALKER
P. PRITCHETT
(INSTITUTE OF GEOHPYSICS
AND PLANETARY PHYSICS):
LIBRARY
C. KENNEL
F. CORONITI

UNIVERSITY OF CHICAGO
ENRICO FERMI INSTITUTE
CHICAGO, IL 60637
E.N. PARKER
I. LERCHE
LIBRARY

UNIVERSITY OF COLORADO
DEPT. OF ASTRO-GEOPHYSICS
BOULDER, CO 80302
M. GOLDMAN
LIBRARY

CORNELL UNIVERSITY
SCHOOL OF APPLIED AND
ENGINEERING PHYSICS
COLLEGE OF ENGINEERING
ITHACA, NY 14853
LIBRARY
R. SUDAN
B. KUSSE
H. FLEISCHMANN
C. WHARTON
F. MORSE
R. LOVELACE
P.M. KINTNER

HARVARD UNIVERSITY
CENTER FOR ASTROPHYSICS
60 GARDEN STREET
CAMBRIDGE, MA 02138
G.B. FIELD
R. ROSNER
K. TSINGANOS
G.S. VAIANA

UNIVERSITY OF IOWA
IOWA CITY, IA 52240
C.K. GOERTZ
D. GURNETT
G. KNORR
D. NICHOLSON
C. GRABBE
L.A. FRANK
K. NISHIKAWA
N. D'ANGELO
R. MERLINO
C. HUANG

UNIVERSITY OF MARYLAND
PHYSICS DEPARTMENT
COLLEGE PARK, MD 20742
K. PAPADOPOULOS
H. ROWLAND
C. WU

UNIVERSITY OF MARYLAND, IPST
COLLEGE PARK, MD 20742
DAVID MATTHEWS

UNIVERSITY OF MINNESOTA
SCHOOL OF PHYSICS
MINNEAPOLIS, MN 55455
LIBRARY
J.R. WINCKLER
P. KELLOGG
R. LYSAK

M.I.T.
CAMBRIDGE, MA 02139
LIBRARY
(PHYSICS DEPARTMENT):
B. COPPI
V. GEORGE
G. BEKEFI
T. CHANG
T. DUPREE
R. DAVIDSON
(ELECTRICAL ENGINEERING
DEPARTMENT):
R. PARKER
A. BERS
L. SMULLIN
(R.L.E):
LIBRARY
(SPACE SCIENCE):
READING ROOM

UNIVERSITY OF NEW HAMPSHIRE
DEPARTMENT OF PHYSICS
DURHAM, NH 03824
R.L. KAUFMAN
J. HOLLWEG

PRINCETON UNIVERSITY
PRINCETON, NJ 08540
PHYSICS LIBRARY
PLASMA PHYSICS LAB. LIBRARY
F. PERKINS
T.K. CHU
H. OKUDA
H. HENDEL
R. WHITE
R. KURLSRUD
H. FURTH
S. YOSHIKAWA
P. RUTHERFORD

RICE UNIVERSITY
HOUSTON, TX 77001
SPACE SCIENCE LIBRARY
T. HILL
R. WOLF
P. REIFF
G.-H. VOIGT

UNIVERSITY OF ROCHESTER
ROCHESTER, NY 14627
A. SIMON

STANFORD UNIVERSITY
RADIO SCIENCE LABORATORY
STANFORD, CA 94305
R. HELLIWELL

STEVENS INSTITUTE OF TECHNOLOGY
HOBOKEN, NJ 07030
B. ROSEN
G. SCHMIDT
M. SEIDL

UNIVERSITY OF TEXAS
AUSTIN, TX 78712
W. DRUMMOND
V. WONG
D. ROSS
W. HORTON

UNIVERSITY OF TEXAS
CENTER FOR SPACE SCIENCES
P.O. BOX 688
RICHARDSON, TX 75080
DAVID KLUMPAR

THAYER SCHOOL OF ENGINEERING
DARTMOUTH COLLEGE
HANOVER, NH 03755
BENGT U.O. SONNERUP
M. HUDSON

UTAH STATE UNIVERSITY
DEPT. OF PHYSICS
LOGAN, UT 84322
ROBERT W. SCHUNK

UNIVERSITY OF THESSALONIKI
DEPARTMENT OF PHYSICS
GR-54006 THESSALONIKI,
GREECE
L. VLAHOS

IONOSPHERIC MODELING DISTRIBUTION LIST
(UNCLASSIFIED ONLY)

PLEASE DISTRIBUTE ONE COPY TO EACH OF THE FOLLOWING PEOPLE (UNLESS OTHERWISE NOTED)

NAVAL RESEARCH LABORATORY
WASHINGTON, DC 20375-5000
DR. S. OSSAKOW, CODE 4700 (2 CYS)
DR. I. VITKOVITSKY, CODE 4701
DR. J. HUBA, CODE 4780 (2 CYS)
DR. H. GURSKY, CODE 4100
DR. J.M. GOODMAN, CODE 4180
DR. P. RODRIGUEZ, CODE 4706
DR. P. MANGE, CODE 1004
DR. R. MEIER, CODE 4140
CODE 2628 (22 CYS)
CODE 1220

A.F. GEOPHYSICAL LABORATORY
L.G. HANSCOM FIELD
BEDFORD, MA 01731
DR. T. ELKINS
DR W. SWIDER
MRS. R. SAGALYN
DR. J.M. FORBES
DR. T.J. KENESHEA
DR. W. BURKE
DR. H. CARLSON
DR. J. JASPERSE
DR. J.F. RICH
DR. N. MAYNARD
DR. D.N. ANDERSON

BOSTON UNIVERSITY
DEPARTMENT OF ASTRONOMY
BOSTON, MA 02215
DR. J. AARONS
DR. M. MENDILLO

CORNELL UNIVERSITY
ITHACA, NY 14850
DR. R. SUDAN
DR. D. FARLEY
DR. M. KELLEY

HARVARD UNIVERSITY
HARVARD SQUARE
CAMBRIDGE, MA 02138
DR. M.B. McELROY

INSTITUTE FOR DEFENSE ANALYSIS
1801 N. BEAUREGARD STREET
ARLINGTON, VA 22311
DR. E. BAUER

MASSACHUSETTS INSTITUTE OF TECHNOLOGY
PLASMA FUSION CENTER
CAMBRIDGE, MA 02139
LIBRARY, NW16-262
DR. T. CHANG
DR. R. LINDZEN

NASA
GODDARD SPACE FLIGHT CENTER
GREENBELT, MD 20771
DR. R.F. PFAFF, CODE 696
DR. R.F. BENSON
DR. K. MAEDA
DR. S. CURTIS
DR. M. DUBIN

COMMANDER
NAVAL OCEAN SYSTEMS CENTER
SAN DIEGO, CA 95152
MR. R. ROSE, CODE 5321

NOAA
DIRECTOR OF SPACE AND
ENVIRONMENTAL LABORATORY
BOULDER, CO 80302
DR. A. GLENN JEAN
DR. G.W. ADAMS
DR. K. DAVIES
DR. R.F. DONNELLY

OFFICE OF NAVAL RESEARCH
800 NORTH QUINCY STREET
ARLINGTON, VA 22217
DR. G. JOINER
DR. C. ROBERSON

LABORATORY FOR PLASMA AND
FUSION ENERGIES STUDIES
UNIVERSITY OF MARYLAND
COLLEGE PARK, MD 20742
JEAN VARYAN HELLMAN,
REFERENCE LIBRARIAN

PENNSYLVANIA STATE UNIVERSITY
UNIVERSITY PARK, PA 16802
DR. J.S. NISBET
DR. P.R. ROHRBAUGH
DR. L.A. CARPENTER
DR. M. LEE
DR. R. DIVANY
DR. P. BENNETT
DR. E. KLEVANS

PRINCETON UNIVERSITY
PLASMA PHYSICS LABORATORY
PRINCETON, NJ 08540
DR. F. PERKINS

SAIC
1150 PROSPECT PLAZA
LA JOLLA, CA 92037
DR. D.A. HAMLIN
DR. L. LINSON

SRI INTERNATIONAL
333 RAVENSWOOD AVENUE
MENLO PARK, CA 04025
DR. R. TSUNODA
DR. WALTER CHESNUT
DR. J. VICKREY
DR. R. LIVINGSTON

STANFORD UNIVERSITY
STANFORD, CA 04305
DR. P.M. BANKS
DR. R. HELLIWELL

U.S. ARMY ABERDEEN RESEARCH
AND DEVELOPMENT CENTER
BALLISTIC RESEARCH LABORATORY
ABERDEEN, MD
DR. J. HEIMERL

GEOPHYSICAL INSTITUTE
UNIVERSITY OF ALASKA
FAIRBANKS, AL 99701
DR. L.C. LEE

UTAH STATE UNIVERSITY
4TH AND 8TH STREETS
LOGAN, UT 84322
DR. R. HARRIS
DR. K. BAKER
DR. R. SCHUNK
DR. J. ST.-MAURICE
DR. N. SINGH
DR. B. FEJER

UNIVERSITY OF CALIFORNIA
LOS ALAMOS NATIONAL LABORATORY
EES DIVISION
LOS ALAMOS, NM 87545
DR. M. PONGRATZ, EES-DOT
DR. D. SIMONS, ESS-7, MS-D466
DR. S.P. GARY, ESS-8
DENNIS RIGGIN, ATMOS SCI GROUP

UNIVERSITY OF ILLINOIS
DEPARTMENT OF ELECTRICAL ENGINEERING
1406 W. GREEN STREET
URBANA, IL 61801
DR. ERHAN KUDEKI

UNIVERSITY OF CALIFORNIA,
LOS ANGELES
405 HILLGARD AVENUE
LOS ANGELES, CA 90024
DR. F.V. CORONITI
DR. C. KENNEL
DR. A.Y. WONG

UNIVERSITY OF MARYLAND
COLLEGE PARK, MD 20740
DR. K. PAPADOPOULOS
DR. E. OTT

JOHNS HOPKINS UNIVERSITY
APPLIED PHYSICS LABORATORY
JOHNS HOPKINS ROAD
LAUREL, MD 20810
DR. R. GREENWALD
DR. C. MENG
DR. T. POTEMRA

UNIVERSITY OF PITTSBURGH
PITTSBURGH, PA 15213
DR. N. ZABUSKY
DR. M. BIONDI

UNIVERSITY OF TEXAS AT DALLAS
CENTER FOR SPACE SCIENCES
P.O. BOX 688
RICHARDSON, TX 75080
DR. R. HEELIS
DR. W. HANSON
DR. J.P. McCLURE

DIRECTOR OF RESEARCH
U.S. NAVAL ACADEMY
ANNAPOLIS, MD 21402
(2 CYS)